AGU PUBLICATIONS

Journal of Advances in Modeling Earth Systems

RESEARCH ARTICLE

10.1002/2016MS000857

Key Points:
- Ensemble superparameterization is used for model uncertainty representation in probabilistic weather prediction
- We compare probabilistic forecasts with stochastic parameterization versus ensemble superparameterization for tropical convective systems
- Nature of convective error growth in a multiscale ensemble modeling framework is studied

Correspondence to:
A. Subramanian,
subramanian@atm.ox.ac.uk

Citation:
Subramanian, A. C., and T. Palmer (2017), Ensemble superparameterization versus stochastic parameterization: A comparison of model uncertainty representation in tropical weather prediction, *J. Adv. Model. Earth Syst.*, *9*, 1231–1250, doi:10.1002/2016MS000857.

Received 8 NOV 2016
Accepted 11 APR 2017
Accepted article online 20 APR 2017
Published online 22 MAY 2017

Ensemble superparameterization versus stochastic parameterization: A comparison of model uncertainty representation in tropical weather prediction

Aneesh C. Subramanian[1] and Tim N. Palmer[1]

[1]Department of Physics, University of Oxford, Oxford, UK

Abstract Stochastic schemes to represent model uncertainty in the European Centre for Medium-Range Weather Forecasts (ECMWF) ensemble prediction system has helped improve its probabilistic forecast skill over the past decade by both improving its reliability and reducing the ensemble mean error. The largest uncertainties in the model arise from the model physics parameterizations. In the tropics, the parameterization of moist convection presents a major challenge for the accurate prediction of weather and climate. Superparameterization is a promising alternative strategy for including the effects of moist convection through explicit turbulent fluxes calculated from a cloud-resolving model (CRM) embedded within a global climate model (GCM). In this paper, we compare the impact of initial random perturbations in embedded CRMs, within the ECMWF ensemble prediction system, with stochastically perturbed physical tendency (SPPT) scheme as a way to represent model uncertainty in medium-range tropical weather forecasts. We especially focus on forecasts of tropical convection and dynamics during MJO events in October–November 2011. These are well-studied events for MJO dynamics as they were also heavily observed during the DYNAMO field campaign. We show that a multiscale ensemble modeling approach helps improve forecasts of certain aspects of tropical convection during the MJO events, while it also tends to deteriorate certain large-scale dynamic fields with respect to stochastically perturbed physical tendencies approach that is used operationally at ECMWF.

Plain Language Summary Probabilistic weather forecasts, especially for tropical weather, is still a significant challenge for global weather forecasting systems. Expressing uncertainty along with weather forecasts is important for informed decision making. Hence, we explore the use of a relatively new approach in using super-parameterization, where a cloud resolving model is embedded within a global model, in probabilistic tropical weather forecasts at medium range. We show that this approach helps improve modeling uncertainty in forecasts of certain features such as precipitation magnitude and location better, but forecasts of tropical winds are not necessarily improved.

1. Introduction

Global atmospheric models have been using subgrid-scale parameterization for more than four decades to represent the wide range of convective processes that occur on horizontal scales smaller than the grid spacing [*Arakawa and Wu*, 2013; *Plant and Yano*, 2015]. Cloud and convection parameterization has proven to be a long-term challenge because of the many processes and many scales involved. Several approaches have been developed to represent atmospheric convection in highly simplified parameterization schemes in global climate models (GCMs) over the past five decades [*Smith*, 2013; *Plant and Yano*, 2015].

The methods to parameterize atmospheric convection can be classified mainly into three complementary approaches, which are termed here as conventional, stochastic, and superparameterization. The most thoroughly established of these approaches is conventional parameterization which parameterize convection as a function of instability parameters of the large-scale fields (scales greater than 50 km) in the model. Conventional parameterizations were first developed in the 1960s [*Smagorinsky*, 1960; *Manabe et al*., 1965; *Kuo*, 1965]. A fundamental assumption with these approaches is that the subgrid tendency are an average over some putative ensemble of subgrid convective elements which are in quasi-equilibrium with the resolved

flow [*Arakawa and Schubert*, 1974]. The review by *Arakawa and Jung* [2011] summarizes work on conventional cumulus parameterizations very well.

Over the last decade, attempts have been made to improve the representation of the multiscale nature of cumulus convection and alleviate some of these drawbacks of conventional parameterization methods through contemporary stochastic mathematical methods. Many previous studies have shown that the statistical properties of a chaotic turbulent cloud system are not completely deterministic [e.g., *Hohenegger et al*., 2006; *Shutts and Palmer*, 2007; *Hohenegger and Schär*, 2007]. Recent work on stochastic parameterizations of deep cumulus convection is aimed at including such nondeterministic effects [*Buizza et al*., 1999; *Lin and Neelin*, 2003; *Shutts and Palmer*, 2007; *Plant and Craig*, 2008; *Peters et al*., 2013; *Deng et al*., 2015; *Khouider and Majda*, 2016; *Wang et al*., 2016] of convection on the large-scale resolved fields in GCMs. The results are intriguing, but further research is needed to establish to what extent stochastic parameterizations are needed for successful simulations of the global circulation of the atmosphere and climate.

An alternative strategy for including the effects of moist convection in numerical models through explicit turbulent fluxes calculated from a cloud-resolving model (CRM) has been developed called superparameterization [*Grabowski and Smolarkiewicz*, 1999; *Grabowski*, 2003; *Randall et al*., 2003]. Superparameterization blends conventional parameterization on a coarse mesh with detailed cloud-resolving modeling on a finer mesh with an imposed scale separation. This method has yielded promising new results regarding tropical intraseasonal behavior [*Khairoutdinov et al*., 2005].

The spatiotemporal scales resolved in a CRM are on the order of 10 km and time of 5 min, with an active moisture and fully nonlinear dynamical field. Strong horizontal and vertical velocities and a fully nonlinear bulk microphysics are allowed [*Lipps and Hemler*, 1982; *Klein and Majda*, 2006]. The computational cost of a superparameterization approach with periodic embedded domains is less than that compared to a high-resolution simulation at a similar resolution as the CRM, as the embedded CRM computations can be done independently at each grid cell and hence is highly parallelizable [*Xing et al*., 2009; *Randall*, 2013; *Arakawa and Jung*, 2011], but still is computationally very expensive.

A further approximation to reduce the cost of the CRM computations is done by reducing the embedded CRM domain to a two-dimensional grid [*Khairoutdinov and Randall*, 2003; *Randall*, 2013]. These approximations have been very successful in not degrading the solutions significantly while reducing the computational cost for convective resolving model solutions. The impact of organized convection through squall lines and mesoscale convective systems [*Moncrieff*, 1992; *Emanuel*, 1994; *Houze*, 2004] on the larger scales is resolved in this framework. Hence, there have been arguments for even more drastic approximations to high-resolution model solutions, which may still produce accurate large-scale solutions [*Xing et al*., 2009; *Majda*, 2007, 2012; *Palmer et al*., 2009a; *Palmer*, 2012, 2014].

One of the major stumbling blocks for GCMs is their poor capability in representing convectively coupled tropical synoptic-scale waves and intraseasonal oscillations such as the Madden-Julian Oscillation (MJO) [*Slingo et al*., 1996; *Lin et al*., 2006; *Kim et al*., 2009]. One conjectured reason for this poor performance is their inadequate representation of interactions across multiple spatiotemporal scales from the convective scale to the circumglobal scale in the tropics. The superparameterization approach has been shown to improve the representation of tropical convection and convectively coupled tropical waves in more than one GCM [*Khairoutdinov et al*., 2005; *Andersen and Kuang*, 2012; *Randall*, 2013]. The strongly nonlinear scales in a CRM with active moisture modify the nonlinear multiscale cascade in a superparameterized model to create the observed statistical self-similarity of tropical convection [*Mapes et al*., 2006; *Majda*, 2007].

Parameterization of convection in GCMs is certainly a source of uncertainty in numerical forecasts, especially in the tropics, which are dominated by deep convective system. Therefore, this uncertainty must be represented explicitly in an ensemble forecast system. Without such a source of uncertainty represented in the ensemble will be under dispersive, where the ensemble spread is lesser than the error in the ensemble mean. The SPPT scheme has been implemented operationally in the European Centre for Medium-Range Weather Forecasts (ECMWF) ensemble prediction system (EPS) to represent the model physics uncertainty, which can largely be attributed to the uncertainty in parameterized convective tendencies in the tropics [*Palmer et al*., 2009b; *Weisheimer et al*., 2014; *Subramanian et al*., 2016]. The SPPT scheme helps improve the reliability of the operational ECMWF EPS both in the extratropics and in the tropics; yet the system is

underdispersive in the tropics [*Palmer et al*., 2009b]. Improvements to the current representation of model uncertainty, especially in the tropical atmosphere, can help improve the reliability of the EPS.

Here we assess the new approach of an ensemble superparameterization (ESP) modeling framework against the conventional SPPT scheme as alternative representations of model uncertainty for tropical weather prediction on timescales from weather to subseasonal ranges. Our approach borrows from the superparameterization approach, where we embed a cloud-resolving model [*Khairoutdinov et al*., 2005] within the ECMWF Integrated Forecasting System (IFS) model. Further details about this model are given in following sections. We test this new modeling framework for tropical weather forecasts, especially during a strong MJO event in 2011. We compare probabilistic forecasts performed using the ESP approach with those using a conventional convection parameterization [*Bechtold et al*., 2008] and a modified version of stochastic physics perturbations, SPPT [*Palmer et al*., 2009b], which is used operationally at ECMWF. We compare and evaluate the ensemble forecasts to understand the nature of model error growth as a function of lead time in forecasts to verify if the ensemble spread captures the growth in forecast error of the ensemble mean in both experiments. For a reliable probabilistic forecast, we would like the ensemble spread to match the root mean square error of the ensemble mean.

The present paper addresses issues about convective error growth through systematic multiscale modeling for the spatiotemporal scales of deep convection. After a preliminary section on the forecasting approach and experiment design in section 2, the main results in the paper are presented in section 3; there it is shown that the ESP modeling approach helps improve forecasting of certain tropical variables, while it also degrades others for numerical weather prediction (NWP). In section 4, there is a discussion of the potential use of the present ensemble superparameterization in designing new strategies for stochastic parameterizations in NWP that retain the fidelity of cloud-resolving modeling with roughly 4 km resolution and a significantly reduced computational overhead compared to a global cloud-resolving models.

2. Modeling and Methods

2.1. Integrated Forecasting System

The model integrations for the ensemble forecasts are performed with the ECMWF IFS at a horizontal resolution of T159 ($\approx$1.125°) and 91 levels in the vertical (between the surface and the 5 hPa level (about 35 km altitude)). The ECMWF IFS model used for all forecasts is a two-time-level semi-Lagrangian global spectral model. The semi-Lagrangian scheme uses a Stable Extrapolation Two-Time-Level Scheme (SETTLS) and a finite element scheme for the vertical discretization. The atmospheric model is coupled to an ocean wave model and to a land-surface model and comprises a comprehensive set of parameterizations for physical processes such as radiative transfer and moist processes. The atmospheric model is coupled to an ocean wave model, an ocean model (NEMO), and a land-surface model (HTESSEL).

The model is triangularly truncated at a spherical harmonics total wave number 159 which is equivalent to a horizontal resolution of about 112.5 km in the tropics. The integration time step is 3600 s. The ensemble used for the forecasts consists of 20 perturbed forecasts and one unperturbed forecast. Ensemble forecasts are at 12 UTC for 10 different start dates starting from 1 October 2011 spaced apart by 5 days until 15 November 2016.

We conduct an ensemble forecast experiment with two sets of runs. One of them uses the conventional convective parameterization with the operational stochastic physics scheme to represent model uncertainty. These sets of runs are called SPPT-IFS hereafter. The other set of runs uses an initially perturbed ESP approach with IFS. These runs are called ESP-IFS hereafter. The current operational medium-range ensemble prediction system at ECMWF includes two schemes to represent model uncertainty, the SPPT scheme and the stochastically perturbed backscatter (SPBS) scheme. The SPPT scheme is based on the *Buizza et al*. [1999] scheme and applies stochastic perturbations in the form of multiplicative noise to the diabatic (parameterized) part of the tendency equations of the prognostic variables [*Palmer et al*., 2009b; *Weisheimer et al*., 2014; *Berner et al*., 2015]. Details about the ESP-IFS and SPPT experiment are described below.

2.2. Superparameterization

The cloud-resolving model (CRM) used in this study is a three-dimensional model developed initially at the Colorado State University described in detail by *Khairoutdinov and Randall* [2003]. This model has been

widely used for many single column model studies [*Khairoutdinov and Randall*, 2003, and references therein] as well as to couple it to global models in a multiscale modeling framework [*Khairoutdinov et al*., 2005; *Randall*, 2013]. The model uses large-scale forcing and surface forcing fields either derived from a processed observational data set (such as the ARM data set [*Ackerman et al*., 2016]) or from GCM grid mean fields.

Although the CRM used in this study does not resolve all the turbulent eddy length scales of cloud-scale dynamics, the governing equations do permit such dynamics to be physically represented. The model solves the anelastic equations of motion and is based largely on a large eddy simulation (LES) model by *Khairoutdinov and Kogan* [1999]. The prognostic thermodynamic variables include the liquid/ice-water moist static energy, the total nonprecipitating water, and the total precipitating water. The model equations are shown in Appendix A. A detailed description of the model dynamic and thermodynamic equations is discussed in *Khairoutdinov and Randall* [2003]. The model is run at a high horizontal resolution (compared to global or regional model grids) of 4 km. The CRM explicitly resolves the mesoscale updrafts and downdrafts in convective overturns, but parameterizes the small-scale ($\leq$4 km) turbulent eddies that play an important role in mediating the cloud entrainment and mixing with the environment. The subgrid-scale model of the CRM uses a 1.5 order turbulence closure based on prognostic turbulent kinetic energy.

In many multiscale modeling approaches, the interior CRM model grid columns are arranged in a zonal or meridional line such that the subgrid model is a two-dimensional representation of the cloud-resolving motions. In our experiments, we oriented the CRM along the zonal direction. We performed certain sensitivity experiments to compare the CRM orientation in IFS and did not see any significant change in solutions with one orientation over the other. This is also consistent with results discussed in *Arakawa and Jung* [2011]. The lateral boundary conditions are periodic with a rigid lid at the top of the model grid that spans all of the troposphere. Newtonian damping is employed in the upper third of the model grid to avoid wave reflections. The boundary layer diffusion and surface flux coupling uses the Monin-Obukhov length-scale similarity.

The model experiments in this study used a horizontal grid spacing of 4 km with 16 adjacent columns. The time step for the model integration is 20 s. The time step of the GCM is 2700 s. The vertical CRM grid had 79 levels collocated with the IFSs grid levels. The vertical CRM grid spacing increases from 50 m near the surface to 500 m above 5 km.

Coupling between the CRMs and IFS is organized as follows. At the beginning of each simulation, the CRM fields in each IFS grid column are initialized by the IFS grid fields. The CRM is called on each IFS time step. The CRM fields are initialized with the CRM fields that were saved at the end of the previous call. The IFS grid mean tendencies updated from the GCM is used as an additional forcing term in the CRM tendency equation. The CRM is thus continuously integrating its equations for the duration of the IFS time step, continuously forced by large-scale tendencies computed by IFS, as in

$$\left[\frac{\partial \phi}{\partial t}\right]_{LS} = \frac{\phi_{LS} - \overline{\phi}}{\Delta t_{LS}}. \tag{1}$$

Here ϕ is a state variable in the CRM and ϕ_{LS} is a state variable in the GCM. The overbar indicates a domain mean over the CRM grid and the brackets indicate the GCM scale for the tendency term. The tendencies passed on from the CRM to the GCM are a domain mean tendency at each time step of the IFS integration. For computational reasons it is convenient to combine the leading-order equations involving microscale temporal fluctuations into essentially a single moist anelastic system with bulk cloud microphysics.

We further use this superparameterization approach to atmospheric modeling in an ensemble forecast mode, where the GCM fields are integrated forward as an ensemble from a certain initial conditions and each GCM grid area has its own CRM embedded within. We further describe the necessity and benefit of doing this in an ensemble setup in the following section.

2.3. Stochastically Perturbed Physical Tendencies (SPPT)

The SPPT scheme is a stochastic parameterization scheme implemented in the ECMWF IFS to represent uncertainty in its physical parameterization tendencies for moisture, heat, and momentum. A detailed description of the history of the scheme from its first design [*Buizza et al*., 1999] to its latest implementation

is presented in *Palmer et al*. [2009b]. In the SPPT scheme, the sum of the physics tendencies of each of the prognostic variables in the model such as temperature, humidity, and momentum is perturbed by a stochastic multiplicative term. The current SPPT scheme has a smooth map of coefficients over space and time and makes use of a spectral pattern generator to define the perturbation coefficients. The scheme uses a univariate distribution for the perturbations that is independent of the variables to be perturbed. The scheme follows equation (2):

$$X_p = (1 + r\mu)X, \tag{2}$$

where X_p is the perturbed tendency variable, $X = u, v, T, q$ are the parameterized tendencies from the deterministic schemes, and $\mu \in [0, 1]$ is the factor used for reducing the perturbation amplitude close to the surface and in the stratosphere, as perturbations in the near-surface regions have undesirable effects on the ocean, land-surface components such as numerical instabilities, while perturbations in the stratosphere are not desired due to the negligible uncertainty in the clear-sky radiation tendencies in the stratosphere.

The perturbation patterns of r have three defined spatiotemporal decorrelation scales and follow an autoregressive model of order 1 (AR1). The three scales of perturbations have characteristic lengths of (i) 500 km and 6 h decorrelation representing the uncertainty in mesoscale processes, (ii) 1000 km and 3 days representing the synoptic-scale uncertainties in physical tendencies, and (iii) 2000 km and 30 days decorrelation representing the uncertainty in the large-scale impact of subgrid-scale physics tendencies. A unique and interesting feature of this stochastic scheme is that the three scales can be combined linearly as two or more independent patterns to account for model errors at different temporal and spatial scales. The variance of each of these stochastic terms is predetermined and represents the magnitude of the uncertainty in each of these scales. The shortest scale is defined to have the largest amplitude of perturbations signifying that the largest uncertainty lies in the mesoscale physical tendencies. The second and third scales have a lower and the lowest variance correspondingly, signifying that these scales which are partially and fully resolved by the model grid-scale dynamics have lower uncertainty.

The amplitude of the variance for each of these patterns has been motivated by results from coarse-graining studies with CRMs [*Palmer et al*., 2009b; *Shutts and Palmer*, 2007]. For instance, *Shutts and Palmer* [2007] showed that the standard deviation of the temperature tendency in a high-resolution cloud-resolving simulation is linearly related to the mean temperature tendency and hence lends support to a multiplicative noise scheme like SPPT for modeling uncertainty in convective parameterizations. Some theories such as *Craig and Cohen* [2006] argue that temperature tendency errors in convective parameterization behave like a Poisson process, where the variance of the tendency is linearly proportional to the mean temperature tendency. This is also shown in numerical results from a more recent coarse-graining study by *Shutts and Pallarès* [2014]. Another recent study by *Watson et al*. [2015] shows that IFS with the multiplicative-noise SPPT scheme reproduces the observed ratio of the standard deviation of convection to the decrease in the mean of convection as the coincident relative humidity and vertical velocity increase. These recent findings imply that though the ECMWF stochastic perturbed parameterization tendency scheme reproduced some of the observed features of convection, it can be improved further, and its benefits in improving the model spread and skill at short and seasonal timescales can be further enhanced.

2.4. Multiscale Ensemble Modeling

Over the past two decades, ensemble forecasting has become established as a technique in NWP to account for uncertainties in model integrations and initial conditions. The history of ensemble prediction is well described in *Lewis* [2005]. Ensemble forecasting was developed with a goal to quantitatively predict the flow-dependent probability density functions of forecast fields. This is limited both by the model uncertainties and the accurate representation of uncertainties in the initial conditions.

The sources of model uncertainties are of two kinds. One is the ill-representation of certain processes and another is the lack of representation of certain processes in the model. The NWP models have been developed at a process level to incorporate a myriad of physical processes as parameterizations. Each of these parameterizations have uncertainties associated with them and hence representing these uncertainties in model integrations accurately helps evolve the uncertainties in weather forecasts [*Leutbecher and Palmer*, 2008, and references therein].

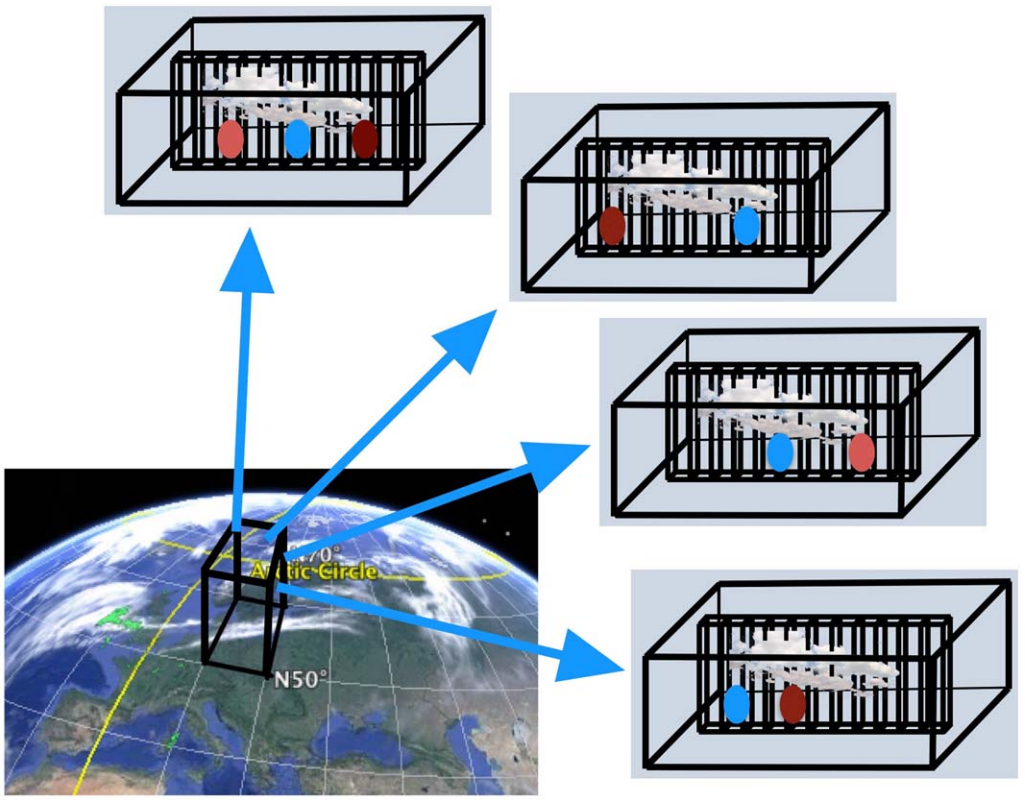

Figure 1. Schematic showing the configuration of the two resolved scales in the superparameterization approach. The outer box represents a single-grid column of the host GCM. The inner boxes represent the interior grid points of the embedded explicit convection model, arranged conventionally in two dimensions, and with a cloud system-resolving model (CSRM) horizontal resolution of several kilometers. The CSRM is then perturbed with a different random perturbation to the temperature in the boundary layer for each ensemble member as depicted by the red and blue ellipses.

We use the ECMWFs medium-range ensemble prediction system (EPS, up to 10 days). The EPS uses initial perturbations from ensemble data assimilation and singular vectors operationally. Yet for the experiments in this study we do not use any initial condition perturbations on the GCM grid in the ensemble since we are interested in growth of model error terms as a function of lead time in forecasts.

In the superparameterization approach to modeling atmospheric convection, we impose a scale separation at the scale of the CRM embedded at each point of the large-scale domain. The mean variables in the CRM are the tendencies that are passed on to the large-scale grid. This scale separation then lends itself to modeling the error growth of the CRM tendencies while the large-scale tendencies are solved with the deterministic set of equations. We test this paradigm to represent convective error growth in our current experiments and compare it to the operational SPPT approach of representing model physics error.

Few recent studies have argued for a need to incorporate uncertainty in the development of parameterization at the process level [*Plant and Craig*, 2008; *Yano*, 2016; *Berner et al*., 2016], rather than as a bolt-on extra as called so by *Palmer* [2012]. In this vein, we propose modeling uncertainty in deep convection using the superparameterization approach as a process level uncertainty modeling framework. In the current set of experiments, we only model the uncertainty in the initial conditions of the CRM with perturbations to the temperature field in the boundary layer. The bottom five layers of the CRM grid cells are perturbed with a $\pm 0.5^{\circ}$C multiplied by a Gaussian random number with no correlation in time or space at the first time step. The IFS grid variables are unperturbed in the ensemble setup at the initial time step. Hence, every ensemble member has exactly the same initial conditions, while the subgrid CRM has perturbed different initial conditions in each ensemble member. A representation of this is shown in Figure 1, where the GCM grid is shown to have different CRMs embedded within for each ensemble member. Integrating this forward for a 10 day forecast then evolves the convective field in the CRMs differently for different ensemble members, which then perturbs the GCM fields differently for each ensemble member and this feedback evolves the

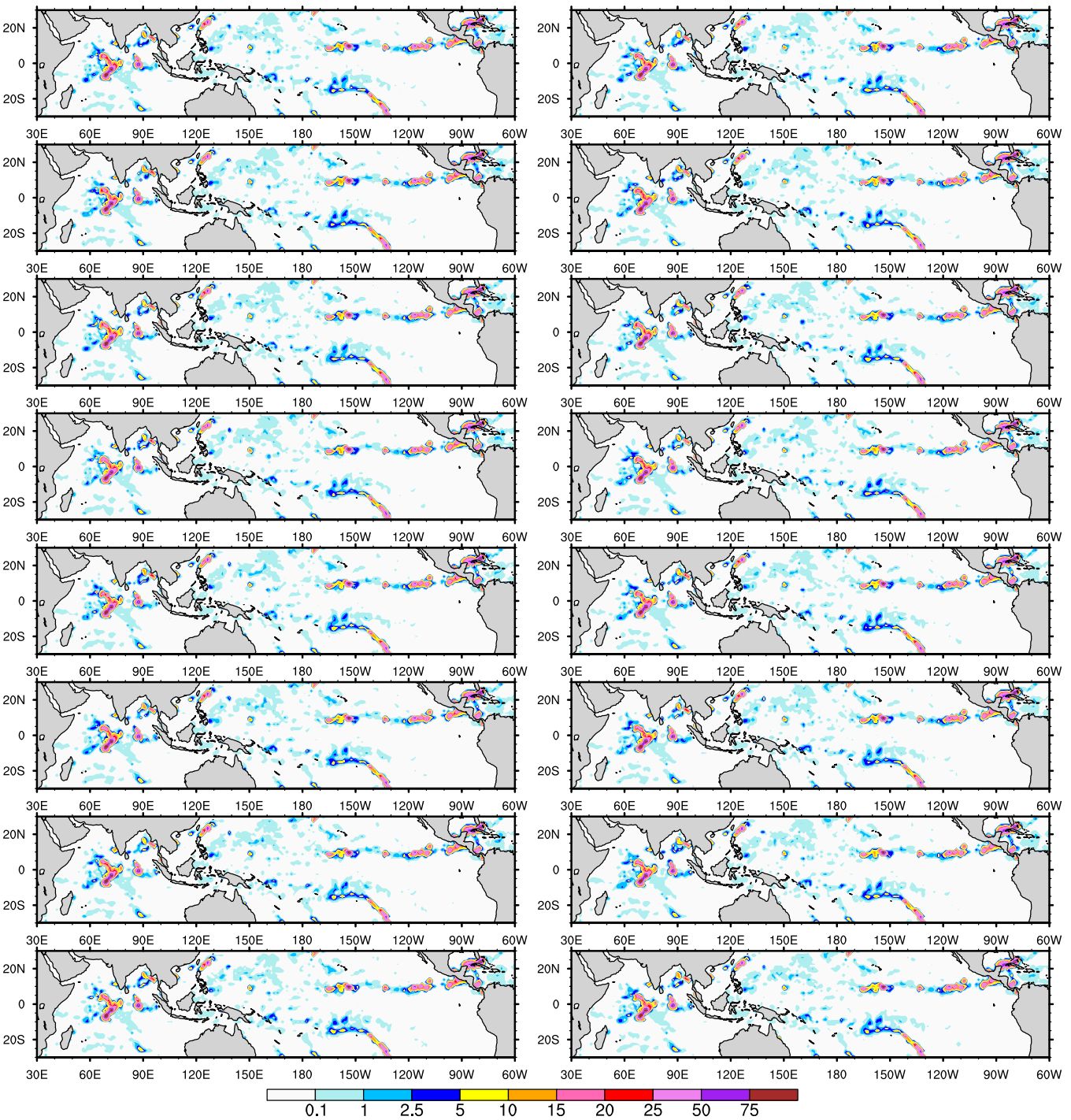

Figure 2. Precipitation field (mm/d) "stamp maps" over the Indian Ocean region of ensemble members for the 24 h ECMWF ESP IFS forecast initialized on 21 October 2011.

uncertainty in the large-scale field driven by uncertainty in the convective field. The results and discussion are presented in following sections.

3. Results

3.1. Convection and the MJO

Figure 2 shows a stamp map of the precipitation field after a 1 day forecast for 16 of 21 ensemble members for the start date of 21 October 2011 for the ESP-IFS run. The large-scale organization of convection and

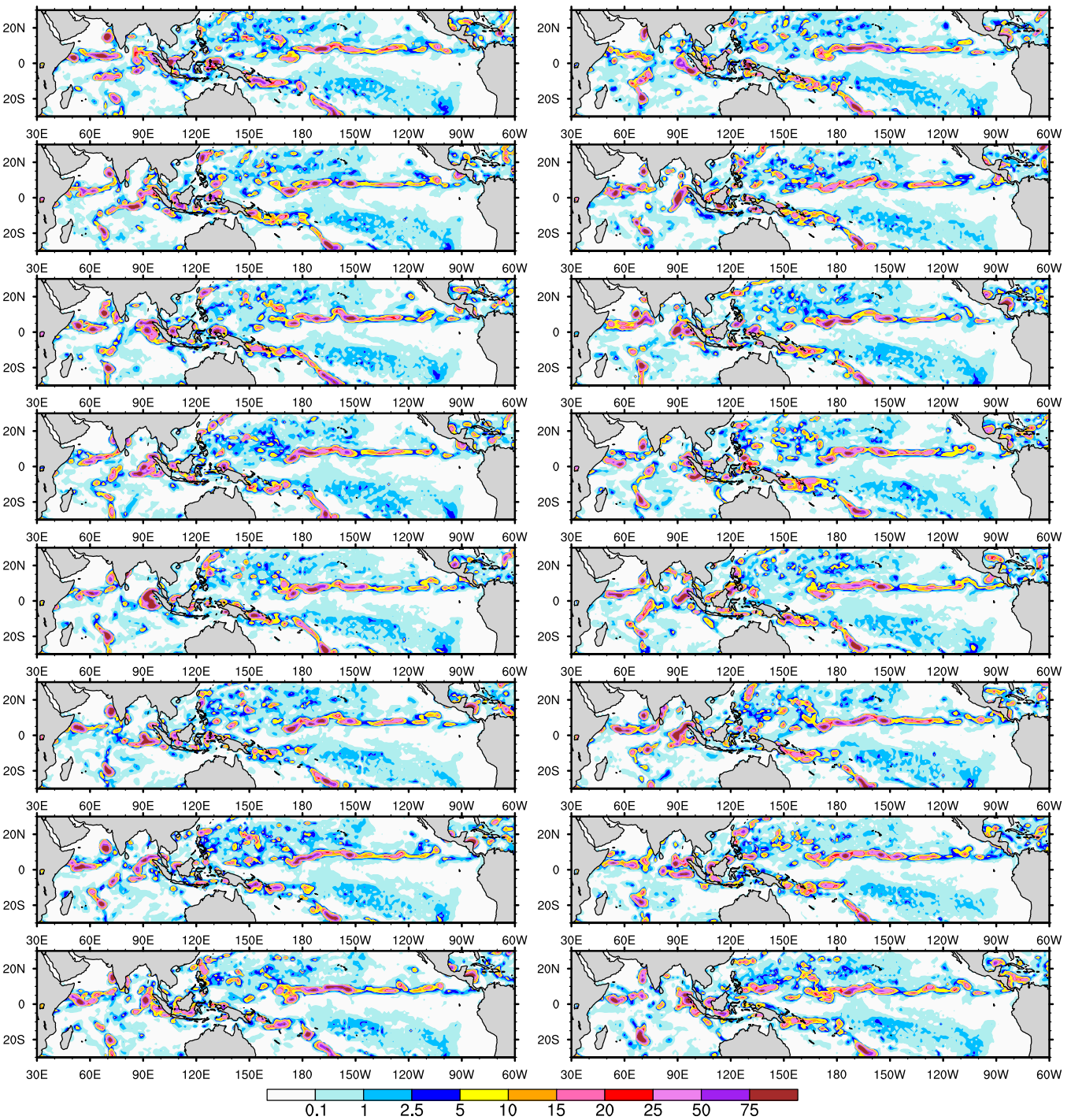

Figure 3. Precipitation field (mm/d) "stamp maps" over the Indian Ocean region of ensemble members for the 240 h ECMWF ESP IFS forecast initialized on 21 October 2011.

precipitation in the Western Indian Ocean region for this case shows the MJO straddling the equator. The precipitation fields do not show much difference among the members after Day 1 forecast. This indicates that the spread in the ensembles for the precipitation field after a 24 h forecast is not very significant qualitatively. We quantify the spread later for many different forecasts. Figure 3 shows the stamp map for the precipitation field in the ESP-IFS experiment after Day 10 forecast for 16 ensemble members for the same start date of 21 October 2011. Here we see a much larger difference among the members in terms of amplitude and location of convection and precipitation. We further quantify the absolute error of the ensemble

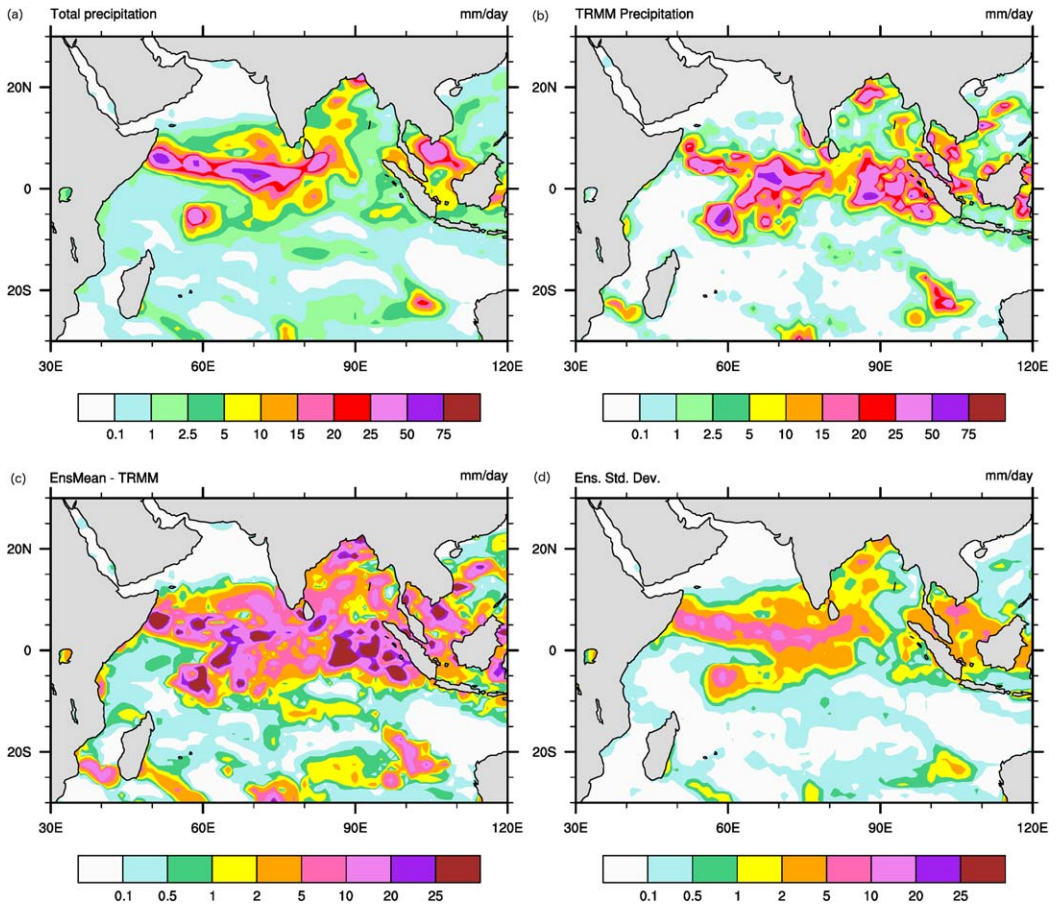

Figure 4. (a) Ensemble mean precipitation in the Tropical Indian ocean region for SPPT-IFS ensemble and (b) TRMM satellite precipitation. Figure 4a is for a 24 h forecast of rainfall in the region. Figure 4c is the absolute error in precipitation compared to TRMM precipitation regridded to model grid. Figure 4d shows the ensemble standard deviation in precipitation. The ensemble forecast was initialized on 21 October 2011.

mean precipitation and Root Mean Square Error (RMSE) of the dynamic fields to compare it with the ensemble spread in these fields.

Figure 4 shows the absolute error and standard deviation in a 24 h forecast of precipitation for the SPPT-IFS experiment compared to TRMM satellite precipitation fields [*Huffman et al.*, 2007] for forecasts initialized on 21 October 2011. Figure 5 shows the same for the ESP-IFS experiment. The absolute error is computed as the absolute difference between the IFS precipitation field and TRMM precipitation fields. The ensemble standard deviation for a 24 h forecast with a SPPT-IFS ensemble shows higher standard deviation values as compared to the ESP-IFS ensemble in many of the regions. Yet by Day 10 forecast (Figure 6) of the SPPT-IFS ensemble, the standard deviation in precipitation saturates to a value lower than the absolute error in the precipitation field over the MJO active region in the Indian Ocean domain. Hence, the SPPT-IFS ensemble forecast has become unreliable in precipitation forecast by Day 10 as the ensemble forecast spread at this lead time does not capture the ensemble mean error from observations. The ensemble standard deviation for the ESP-IFS ensemble forecast for Day 10 (Figure 7) shows higher values of standard deviation in the regions of high convection and precipitation. Here the ESP-IFS ensemble forecast has higher reliability than the SPPT-IFS ensemble forecast as the ensemble spread is closer to the ensemble mean error at Day 10.

In order to understand the differences between the representations of the MJO convection in the two systems, we further analyze the moist static energy (MSE) in the two systems. Recent theoretical and modeling studies have shown that the MJO convection is primarily determined by column latent heat anomalies, which are roughly equivalent to MSE anomalies under a weak temperature gradient assumption [*Charney*,

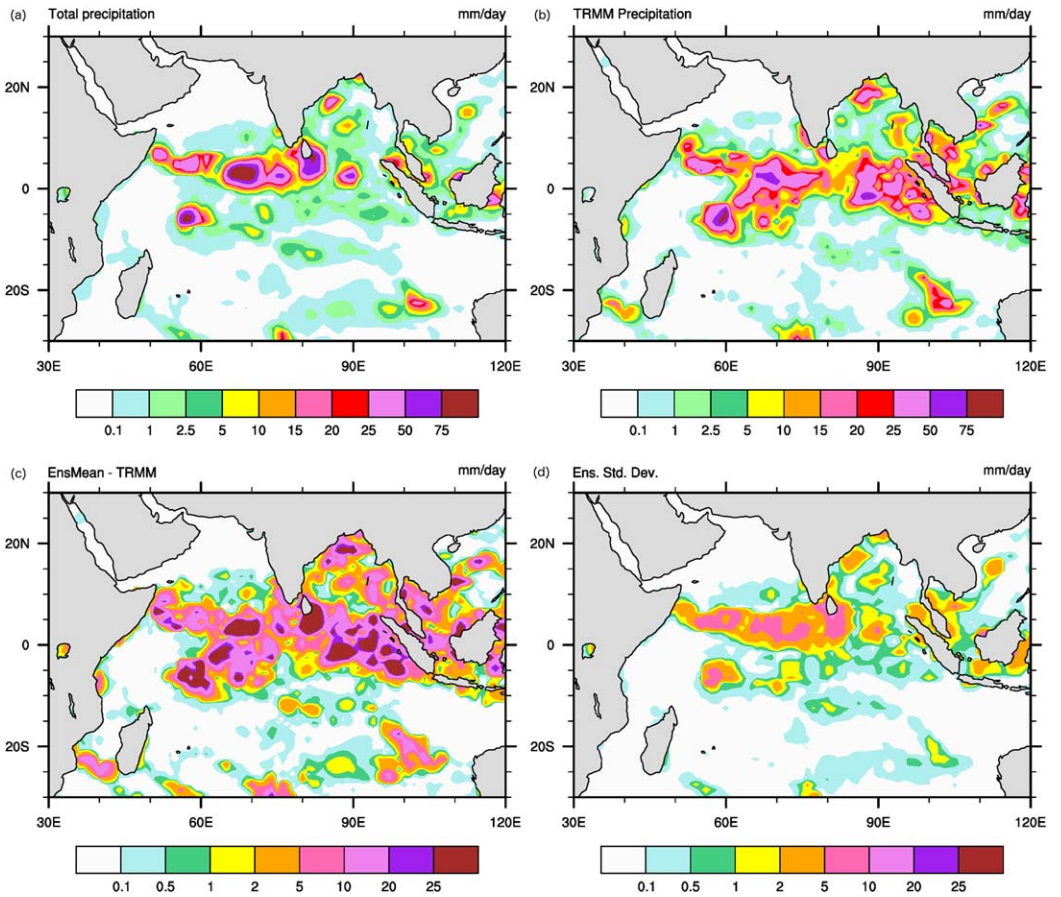

Figure 5. (a) Ensemble mean precipitation in the Tropical Indian ocean region for ESP IFS ensemble and (b) TRMM satellite precipitation. Figure 5a is for a 24 h forecast of rainfall in the region. Figure 5c is the absolute error in precipitation compared to TRMM precipitation regridded to model grid. Figure 5d shows the ensemble standard deviation in precipitation. The ensemble forecast was initialized on 21 October 2011.

1963; *Sobel et al*., 2001] in the tropics, leading to the hypothesis that the MJO is fundamentally a moisture mode [*Raymond and Fuchs*, 2009; *Maloney*, 2009; *Sobel and Maloney*, 2013; *Hannah and Maloney*, 2014], which is also known as the moisture mode theory. A related and compatible theory, the recharge-discharge theory, is that the MJO convection and column MSE in the tropics are strongly related [*Hendon and Liebmann*, 1990; *Blad and Hartmann*, 1993; *Hu and Randall*, 1994; *Maloney*, 2009; *Andersen and Kuang*, 2012; *Subramanian and Zhang*, 2014]. This theory proposes that the MJO convection is regulated by a recharge-discharge cycle, where the column MSE builds up before the MJO deep convection creates precipitation and discharges the MSE. There are subtle differences between the two theories; the moisture mode theory proposes that the MJO convection instead of acting to discharge moisture and MSE anomalies in the tropics helps sustain and enhance the moisture anomalies against the drying effect of horizontal advection. Hence, MJO convection helps maintain the instability in the atmosphere [*Wolding and Maloney*, 2015]. The MSE (denoted in literature as h) in our analysis is defined as

$$h = c_p T + gZ + Lq, \tag{3}$$

where T is the temperature, c_p is the specific heat at constant pressure, Z is the height, g is the gravitational acceleration, L is the latent heat of vaporization, and q is the specific humidity. As constructed the MSE is a conserved quantity subject to removal or addition of liquid water into the column, under hydrostatic motion in the column. Hence, the column-integrated h, $\langle h \rangle$, is approximately conserved. The model tends to conserve this quantity under convective adjustment. The mass-weighted integral of MSE is defined as

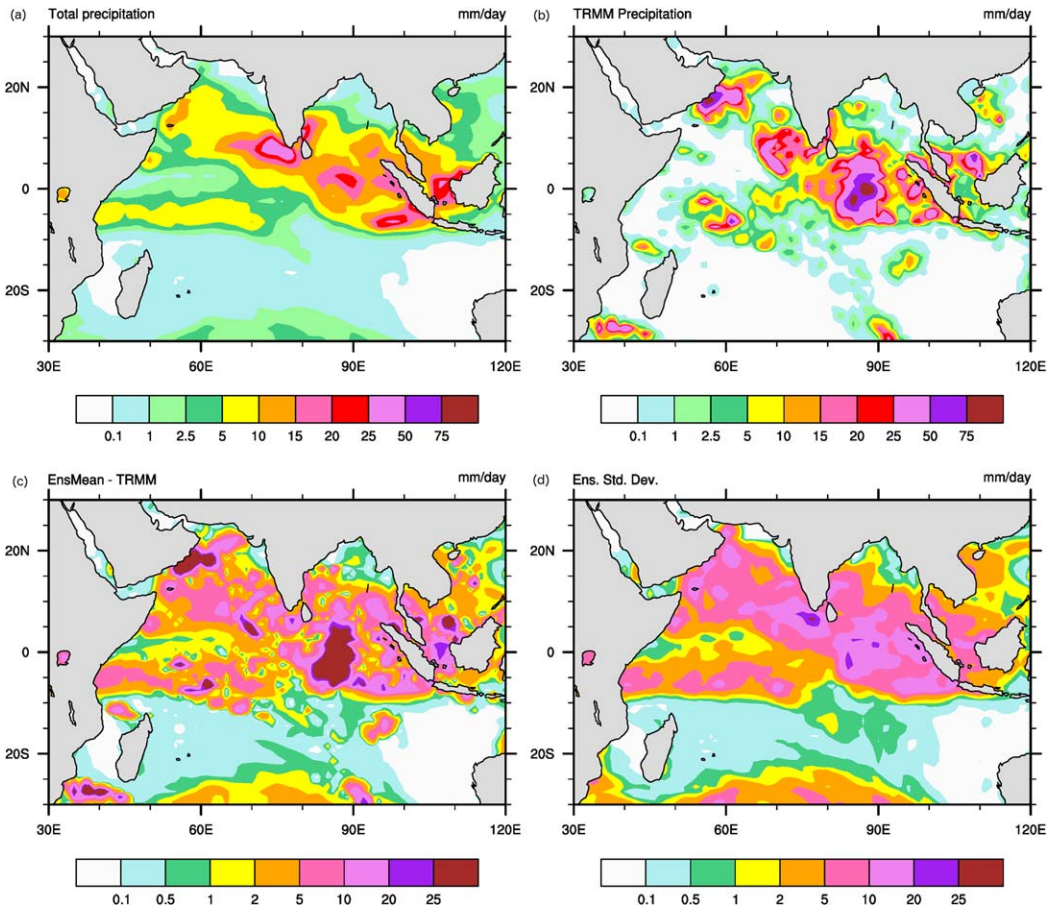

Figure 6. (a) Ensemble mean precipitation in the Tropical Indian ocean region for SPPT-IFS ensemble and (b) TRMM satellite precipitation. Figure 6a is for a 240 h forecast of rainfall in the region. Figure 6c is the absolute error in precipitation compared to TRMM precipitation regridded to model grid. Figure 6d shows the ensemble standard deviation in precipitation. The ensemble forecast was initialized on 21 October 2011.

$$\langle h \rangle = \frac{1}{g} \int_{p_{top}}^{p_{surface}} h dp, \tag{4}$$

where the vertical integral is computed from the top of the atmosphere (or approximately thereof) to the surface. g is the gravitational acceleration and p is the pressure field. The terms that lead to nonconservation of the MSE field are usually negligible compared to the energy budget terms [*Neelin and Held*, 1987].

We study this relationship of the MSE to the MJO convection and precipitation in this ensemble forecast experiment. Looking at the ensemble mean MSE field for the SPPT-IFS experiment and the ESP-IFS experiment in Figure 8, we see that the strong regions of convection and precipitation in the central Indian Ocean region and west Pacific are regions of weak MSE compared to the surrounding regions, since the convection and precipitation discharges the column MSE, after the buildup. The SPPT-IFS shows weaker column-integrated MSE amplitude compared to the maximum amplitude of column MSE in the ESP-IFS experiment. This is also consistent with the ESP-IFS having a more intense but localized precipitation pattern as seen in Figures 8c and 8d as well as in Figures 4a and 5a. The stronger buildup of MSE in the ESP-IFS experiment is likely due to the reduced drizzle or weak amplitude precipitation, which otherwise discharges the column MSE in the SPPT-IFS experiment and hence does not allow for strong buildup of MSE.

This is also true for the MJO convection and MSE for the Day 10 forecast seen in Figure 9. Here the MJO convection has moved to the east Indian ocean region, with strong deep convection and precipitation discharging the MSE in this region. The ESP-IFS experiment shows a net higher-amplitude MSE in the column over the tropical region, both in the Indian Ocean and the West Pacific region. Similar studies with the

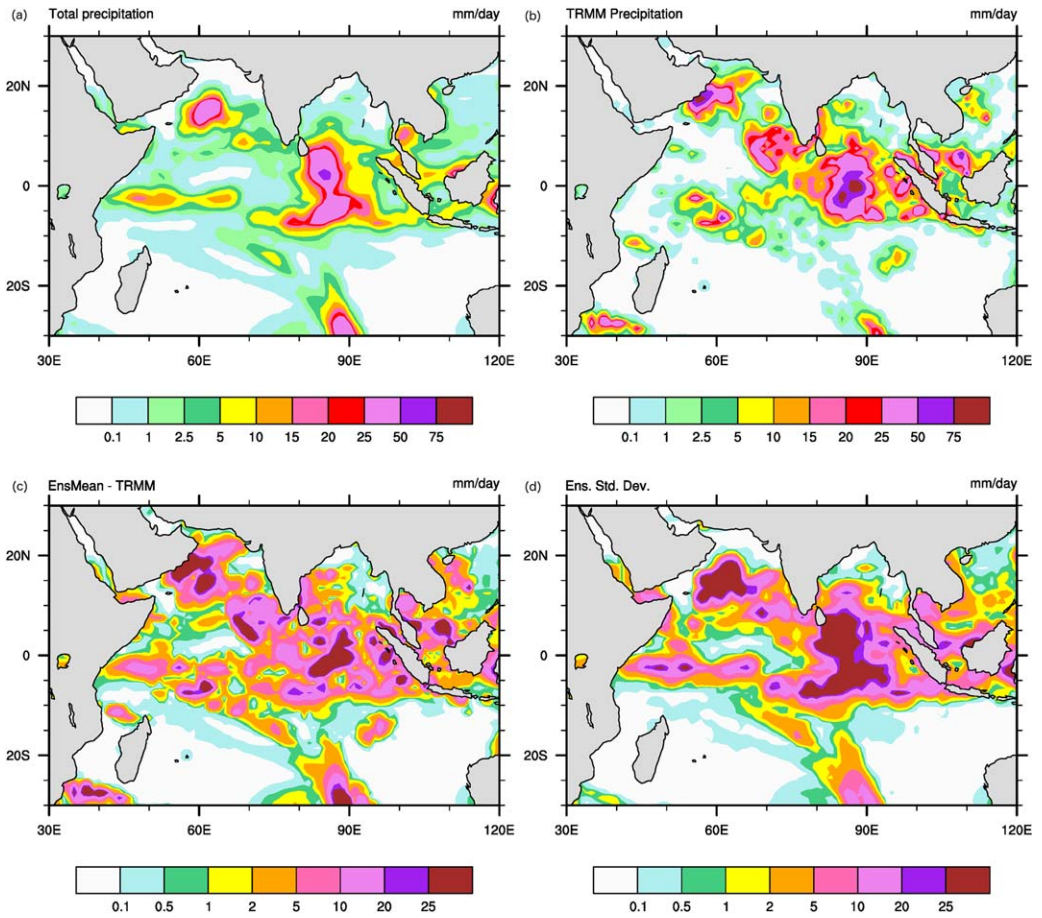

Figure 7. (a) Ensemble mean precipitation in the Tropical Indian ocean region for ESP IFS ensemble and (b) TRMM satellite precipitation. Figure 7a is for a 240 h forecast of rainfall in the region. Figure 7c is the absolute error in precipitation compared to TRMM precipitation regridded to model grid. Figure 7d shows the ensemble standard deviation in precipitation. The ensemble forecast was initialized on 21 October 2011.

superparameterization scheme in the Community Atmosphere Model (CAM) previously have shown that SPCAM tends to build up MSE in the column from horizontal and vertical advection of MSE ahead of the MJO peak in convection during MJO propagation [*Andersen and Kuang*, 2012]. The deep convection and precipitation act to reduce the column MSE as the MJO propagates through the domain.

The ensemble standard deviation in the MSE field and the precipitation for the two experiments are shown in Figures 10 and 11 for Day 1 and Day 10 forecast, respectively. Figures 10 and 11 (top) show the ensemble spread (for SPPT-IFS and ESP-IFS, respectively) in MSE. Figure 10 shows that the spread in the MSE field for the ESP-IFS experiment is of lower amplitude and in smaller regions compared to the MSE spread in the SPPT-IFS experiments. This is also consistent with larger spread in the precipitation field (Figures 10c and 10d) for the SPPT-IFS experiment compared to the ESP-IFS experiment. For the 10 day forecast shown in Figure 11, the spread in the MSE field for the ESP-IFS experiment is larger than that in the SPPT-IFS case in the tropical belt, especially over the MJO convection region in the east Indian Ocean as well as the ITCZ and SPCZ regions. This is also consistent with the increased spread in the precipitation field for the ESP IFS experiment in the Day 10 forecast fields. The spatial pattern of the larger spread in the precipitation for the ESP-IFS experiment indicates that the difference in convection among the ensemble members is mainly in regions of MSE discharge. Hence, in these regions the CRM convection and contribution to the large-scale tendency varies widely among the ensemble members compared to the parameterized tendency differences in the SPPT-IFS experiment. We further investigate this increase in spread of the MSE and the precipitation fields as a function of the components that make up the MSE field and in terms of probabilistic verification metrics.

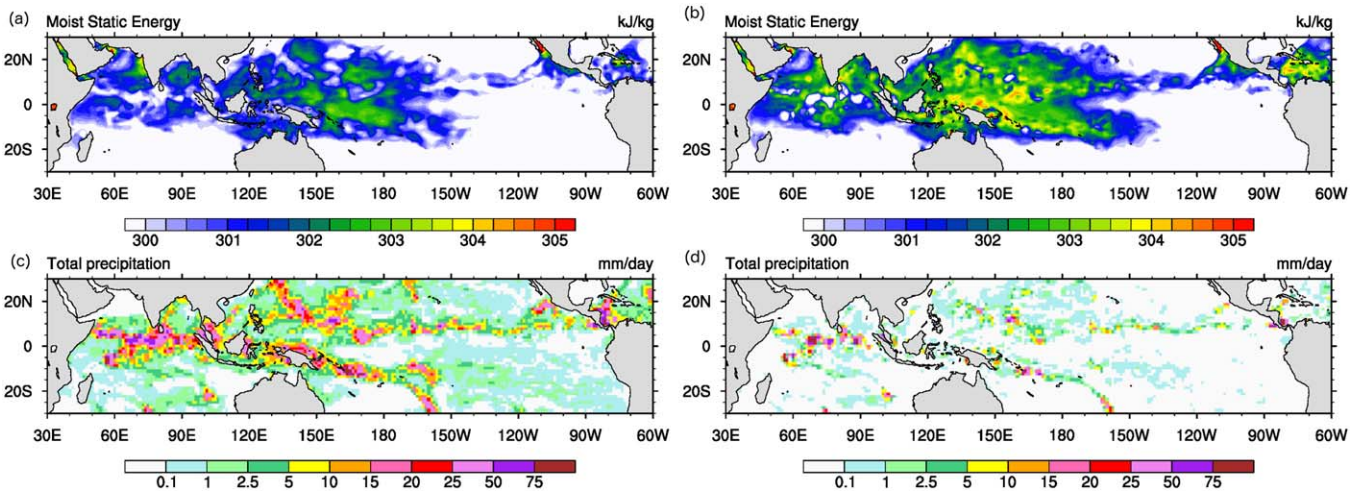

Figure 8. Ensemble mean moist static energy for Day 1 forecast starting on 21 October 2011 for (a) SPPT-IFS ensemble forecast and (b) ESP-IFS ensemble forecast. Ensemble mean precipitation forecast for Day 1 for (c) SPPT-IFS ensemble forecast and (d) ESP-IFS ensemble forecast.

3.2. Ensemble Verification

Figure 12 shows the ensemble standard deviation and ensemble mean root mean square error (RMSE) for the moist static energy field in the Indian ocean region (left; 60°E–100°E and 10°S–10°N) and the West Pacific region (right; 125°E–150°E and 10°S–10°N) for the two experiments ESP-IFS (blue) and SPPT-IFS (red). The ensemble spread for the MSE field in the ESP-IFS experiment is larger than that in the SPPT-IFS experiment after Day 6 in both the Indian Ocean (IO) region and the West Pacific (WP) region.

In the IO region, the RMS error for the ESP-IFS experiment saturates and stays below the RMS error for the SPPT-IFS experiment after Day 4. Over the WP region, the ensemble spread of the ESP-IFS experiment is higher than that in the SPPT-IFS experiment after Day 6, while the RMS error of the ensemble mean is lower after Day 7. Hence, the ESP-IFS ensemble prediction system is slightly more skillful than the SPPT-IFS experiment to predict the ensemble mean MSE field as well as the associated uncertainty in this forecast for the extended medium-range period beyond Day 5 in both the basins. Here the ESP-IFS gives a more skillful forecast on these timescales as the ensemble spread captures the error in the ensemble mean better than the SPPT-IFS.

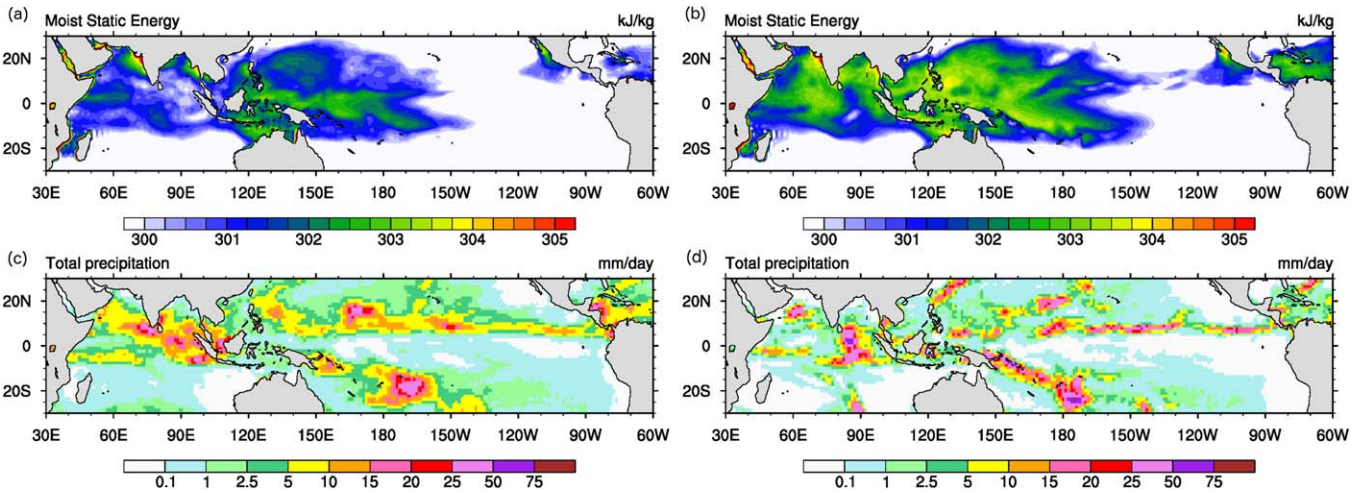

Figure 9. Ensemble mean moist static energy for Day 5 forecast starting on 21 October 2011 for (a) SPPT-IFS ensemble forecast and (b) ESP-IFS ensemble forecast. Ensemble mean precipitation forecast for Day 5 for (c) SPPT-IFS ensemble forecast and (d) ESP-IFS ensemble forecast.

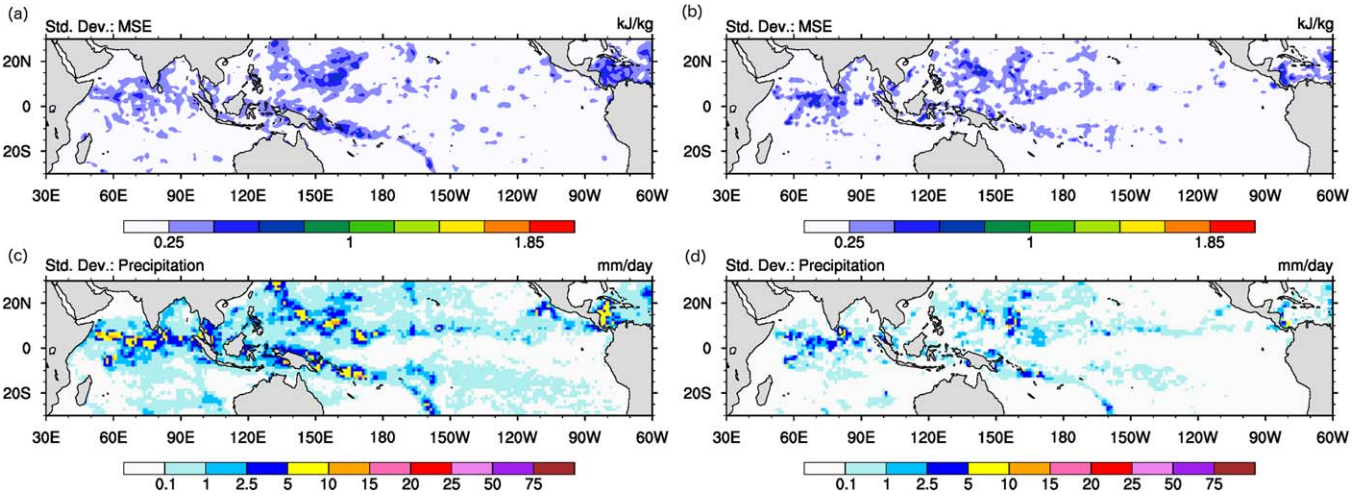

Figure 10. Ensemble spread in moist static energy for Day 1 forecast starting on 21 October 2011 for (a) SPPT-IFS ensemble forecast and (b) ESP-IFS ensemble forecast. Ensemble spread in precipitation forecast for Day 1 for (c) SPPT-IFS ensemble forecast and (d) ESP-IFS ensemble forecast.

We further investigate if this improved skill in predicting the MSE field over the Indian Ocean is due to the improved humidity or temperature field in the region. We analyze the IO region mainly as the MJO convection is active over the IO region during this forecast period. Figure 13 shows the ensemble standard deviation and ensemble mean RMS error for the specific humidity and temperature fields over the Indian Ocean region at two different pressure levels (500 and 850 hPa). The top two figures show the diagnostics for the 500 hPa levels. At both levels it is evident that the forecast ensemble spread is larger in the ESP-IFS experiment for the specific humidity field after Day 4, while the SPPT-IFS experiment has a larger spread in the temperature field. The ESP-IFS ensemble has a RMSE to ensemble spread ratio closer to one at longer lead times compared to that of the SPPT-IFS for the humidity forecast field, despite the RMSE of the humidity field at these two levels being higher. The main difference between how these moisture and temperature tendencies are computed for the ESP-IFS and SPPT-IFS is that the cloud-resolving model in the ESP-IFS approach computes the convective tendencies, while in the SPPT-IFS approach, this is computed by the convective parameterization and perturbed by multiplicative stochastic noise. Hence the ESP-IFS CRM resolves some of the deep convective tendencies in the subgrid scale while SPPT-IFS parameterizes these subgrid-scale tendencies and perturbs them by a characteristic uncertainty, leading to fundamental differences in these tendencies in the models. The increased spread in the ESP-IFS forecast that matches the

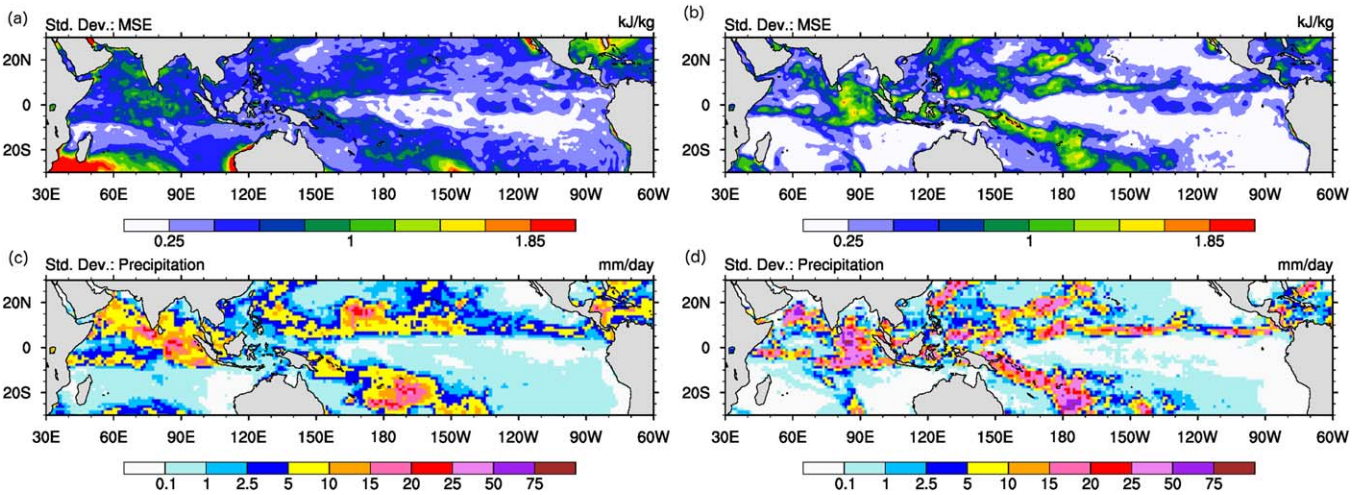

Figure 11. Ensemble spread in moist static energy for Day 5 forecast starting on 21 October 2011 for (a) SPPT-IFS ensemble forecast and (b) ESP-IFS ensemble forecast. Ensemble spread in precipitation forecast for Day 5 for (c) SPPT-IFS ensemble forecast and (d) ESP-IFS ensemble forecast.

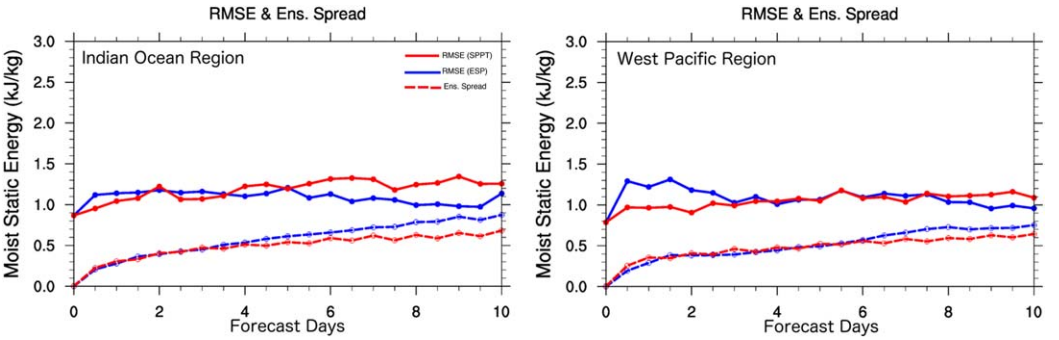

Figure 12. Ensemble standard deviation (dashed lines) and ensemble mean RMS error (continuous lines) for the moist static energy in the Indian Ocean region (left) and West Pacific region (right) for the ESP-IFS (blue line) and for the SPPT-IFS (red line) experiments. These were computed as a mean for 10 different start dates starting from 6 October 2011 until 21 November 2011.

RMSE for the humidity field beyond Day 5 indicates that the ESP-IFS ensemble is more reliable for humidity fields at these longer lead times.

The specific humidity tendencies are largely governed by the convective tendencies in this region, while the temperature tendencies are governed by both the convective physics and the dynamical adjustments. While the radiation scheme in the model modifies the temperature in the column, it does not affect the specific humidity field. Similarly, dry physics schemes can modify the temperature field, while the specific humidity is mainly changed in time due to convection-related physics parameterizations. Hence, we expect this improved probabilistic prediction of the specific humidity field with the superparameterization approach where the growth in mean forecast error of the ensemble mean is captured better by the growth in the ensemble spread for the humidity field.

Recent studies such as *Andersen and Kuang* [2012] and *Arnold et al*. [2013, 2015] argue that the MJO, unlike other convectively coupled equatorial waves, respond to column-integrated MSE anomalies rather than

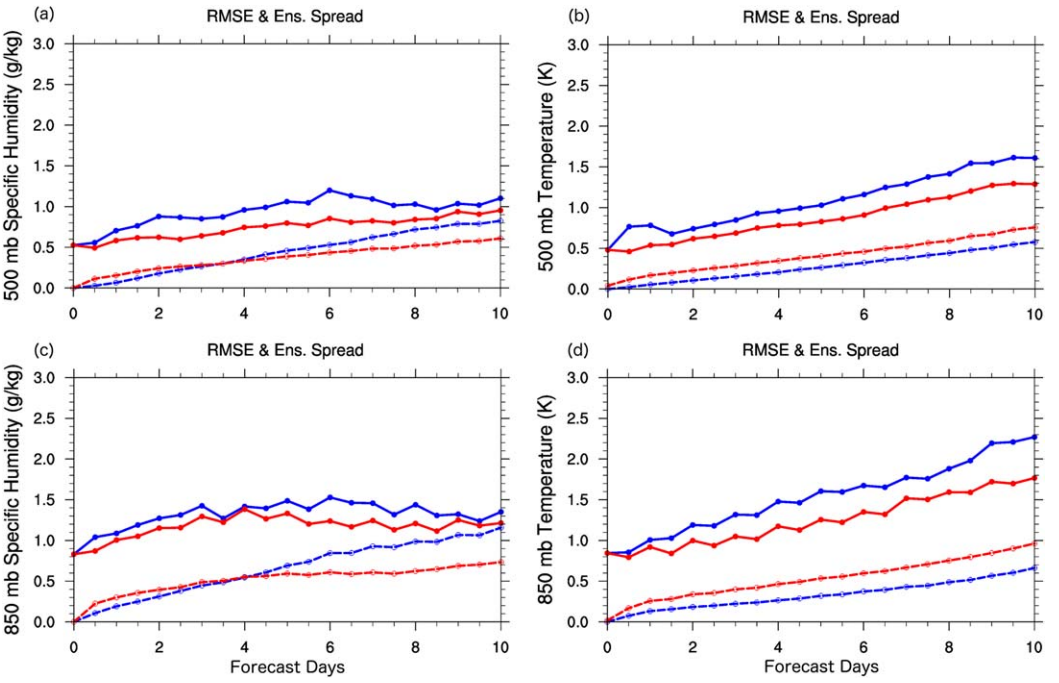

Figure 13. Ensemble standard deviation (dashed lines) and ensemble mean RMS error (continuous lines) for the humidity (left) and temperature (right) at 500 hPa (top) and 850 hPa (bottom) vertical levels over the Indian Ocean region for the ESP-IFS (blue line) and for the SPPT-IFS (red line) experiments. These were computed as a mean for 10 different start dates starting from 6 October 2011 until 21 November 2011.

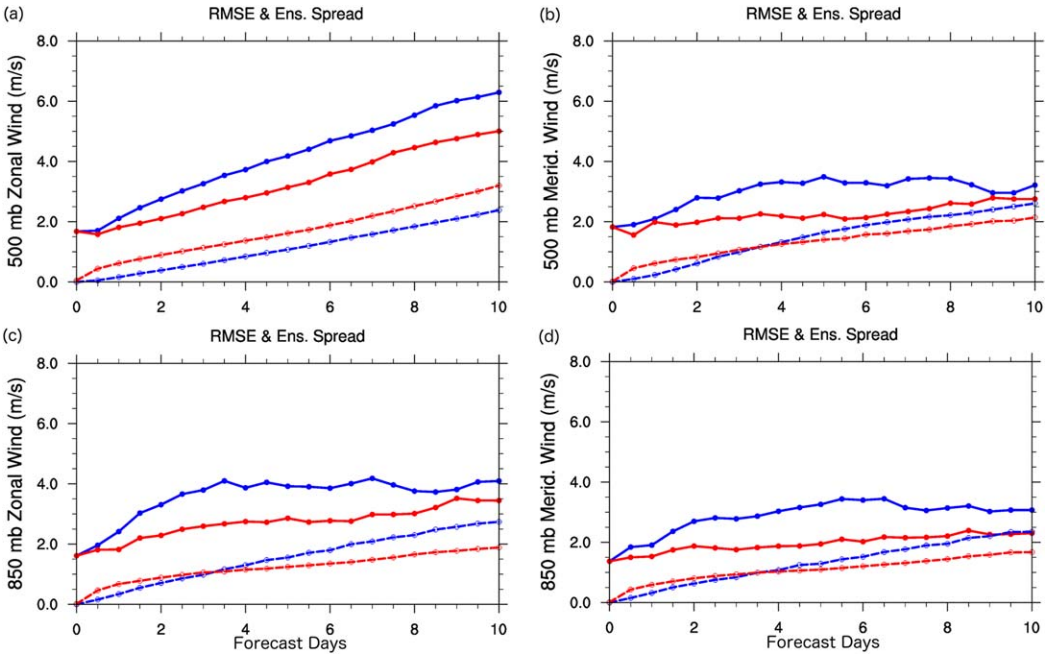

Figure 14. Ensemble standard deviation (dashed lines) and ensemble mean RMS error (continuous lines) for the zonal winds (left) and meridional winds (right) at 500 hPa (top) and 850 hPa (bottom) pressure levels over the Indian Ocean region for the ESP-IFS (blue line) and for the SPPT-IFS (red line) experiments. These were computed as a mean for 10 different start dates starting from 6 October 2011 until 21 November 2011.

convective instabilities due to convective available potential energy. Moist static energy anomalies being predicted more accurately will likely help improve model predictions of the MJO convection. Yet if the temperature field and other relevant dynamical fields in the tropics are poorly predicted, it will lead to a degradation in overall predictive scores of the ensemble prediction system.

Figure 14 shows the ensemble standard deviation and ensemble mean RMS error for the zonal and meridional wind fields at 500 and 850 hPa pressure levels in the top and bottom figures, respectively. This is again computed in the tropical Indian Ocean region. The RMS error for the ensemble mean fields of both zonal and meridional winds in this region is higher for the ESP-IFS experiment over all lead time. The ensemble spread tends to increase more with the ESP-IFS after Day 4 in the meridional wind fields at both levels and the zonal winds at the lower tropospheric level. This is likely due to the improved convection field, which drives low-level convergence into the region. The SPPT-IFS experiment tends to show a more reliable forecast of the mid-tropospheric level zonal winds, as well as for the temperature field in both the lower and midtropospheric levels. We see a similar decrease in probabilistic skill (continuous rank probability skill) metrics for zonal winds and temperature in the tropics for the ESP-IFS forecast runs compared to the SPPT-IFS experiment.

In summary, we find that the ESP approach improves probabilistic forecasts of precipitation and atmospheric humidity fields (especially related to deep convection) while it also degrades the reliability of the ensemble for other fields. The SPPT scheme tends to have a high reliability over the midlatitude region as shown by *Palmer et al*. [2009a, and references therein] and for the temperature and wind fields over the tropics as seen in this study. A fundamental difference between the SPPT approach and the ESP approach is that the SPPT approach tends to perturb the total physics tendencies after all the physics schemes have operated on the model fields, while the ESP approach tends to only evolve the model uncertainty through the deep convection process and therefore represents only a part of the model uncertainty.

4. Conclusions and Discussion

Weather predictions are strongly sensitive to initial condition errors. Ensemble predictions systems have been developed over the past three decades to forecast such flow-dependent predictability. In addition to

initial condition uncertainty, the errors in our formulation of the weather forecasting models add to forecast uncertainty in ensemble forecasts. Representing this model error well is essential for the ensemble prediction system to be reliable in a probabilistic sense. These probabilistic forecast systems with improved reliability have added more value to the weather-related decision-making process than a single deterministic forecast with no quantification of uncertainty.

The largest errors in weather and climate models come from the physics parameterization, especially from the parameterization of subgrid atmospheric convection. Quantifying and representing the uncertainty in the parameterized tendencies of subgrid convection in large-scale models can help improve the ensemble prediction of not only tropical convection but also their teleconnection into global weather patterns. We have compared the conventional SPPT method of representing physics uncertainty with that of an ESP approach and evaluated the reliability of the two probabilistic forecast systems.

The spatial and temporal-scale differences between the CRM and the GCM inherently assumes a separation in scales of the motions in these two regimes, though coupled with each other at the temporal and spatial scales of the large-scale model. The CRM model has "convective memory" as it is initialized by the state of the small-scale CRM variables at the end of the previous time step of the large-scale equations. This is in contrast to conventional convective parameterization schemes, which do not propagate any subgrid-scale convective features in time. Yet approximations such as periodicity in the subgrid domain and two-dimensional grid of the CRM are strong unjustified approximations and can lead to error in computations of convective adjustment.

In this study, we use the superparameterization approach to study error growth in convective processes and large-scale convective phenomena such as the MJO making use of this scale separation for perturbed forecasts. We examined medium-range forecasts over a one and half month period in 2011, which was characterized by strong MJO activity in the tropics. We performed these forecast experiments with two different ensemble forecasting approaches. One of them used the operational stochastic physics scheme known as the SPPT scheme, while the other approach was developed and tested for this study and is called the ensemble superparameterization approach, ESP.

The ESP approach helps improve probabilistic forecasts of tropical deep convection and fields related to the MJO in these forecasts compared to the SPPT approach. The ESP approach uses a cloud-resolved model coupled to the large-scale global model and can be viewed as an ensemble multiscale modeling approach to ensemble weather forecasts. In this framework, we stochastically perturb the boundary layer temperature fields in the CRM and integrate an ensemble of these GCMs forward in time, letting the CRM evolve the convective uncertainty forward in time.

These results indicate that the ESP approach helps improve some aspects of the probabilistic prediction of tropical convection such as precipitation forecasts, the specific humidity field, and the moist static energy variable which is tightly linked to deep convection in the tropics. Yet it also degrades the forecasts of other variables such as temperature and zonal winds. We have shown that the improvement in the precipitation field and hence the representation of convection in the model is largely due to the improvement in ensemble prediction of the humidity field.

This technique of an ensemble multiscale modeling, especially in an ensemble forecasting system, is relatively new and understanding the pros and cons of such a technique is very useful in terms of determining the benefits and drawbacks of the SPPT scheme. This is especially true for understanding the error growth time and spatial scales for convection as compared to a holistic scheme such as SPPT with prescribed temporal and spatial scales. We hope to understand better the error growth from the convective scales to the large scales and hence help improve the representation of model error growth in SPPT-like holistic and computationally cheaper schemes. Sensitivity of the error growth to representation of uncertainty in the microphysics parameterization of the CRMs are also of interest, as these are the subgrid-scale parameterizations in the CRMs. Understanding the sensitivity to cloud microphysics could point us to representing model uncertainties when we have a convection permitting global ensemble.

The success of ensemble multiscale modeling in the current study, which is analogous to more advanced stochastic techniques such as the stochastic superparameterization presented in previous studies [*Grooms and Majda*, 2013; *Majda et al*., 2008; *Grooms and Majda*, 2014; *Grooms et al*., 2015; *Deng et al*., 2015],

supports further studies into understanding and modeling subgrid-scale uncertainty evolution with more physically based approaches. We recommend future studies to explore physical methods to help understand the nature of error growth in subgrid-scale processes such as convection or turbulent mixing. This will help inform the design of next generation stochastic modeling approaches in convection-resolving global models.

Appendix A: The CRM Equations

The anelastic momentum conservation equations solved in the CRM integration are described here in tensor notation,

$$\frac{\partial u_i}{\partial t} = -\frac{1}{\overline{\rho}}\frac{\partial}{\partial x_j}(\overline{\rho} u_i u_j + \tau_{ij}) - \frac{\partial}{\partial x_i}\frac{p'}{\overline{\rho}} + \delta_{i3} B + \epsilon_{ij3} f (u_j - U_{gj}) + \left(\frac{\partial u_i}{\partial t}\right)_{l.s.}, \tag{A1}$$

$$\frac{\partial \overline{\rho} u_i}{\partial x_i} = 0, \tag{A2}$$

$$\frac{\partial h_L}{\partial t} = -\frac{1}{\overline{\rho}}\frac{\partial}{\partial x_i}(\overline{\rho} u_i h_L + F_{h_L i}) - \frac{1}{\overline{\rho}}\frac{\partial}{\partial z}(L_c P_r + L_s P_s + L_s P_g), \tag{A3}$$

$$+\left(\frac{\partial h_L}{\partial t}\right)_{rad} + \left(\frac{\partial h_L}{\partial t}\right)_{l.s.}, \tag{A4}$$

$$\frac{\partial q_T}{\partial t} = -\frac{1}{\overline{\rho}}\frac{\partial}{\partial x_i}(\overline{\rho} u_i q_T + F_{q_T i}) - \left(\frac{\partial q_p}{\partial t}\right)_{mic} + \left(\frac{\partial q_p}{\partial t}\right)_{l.s.}, \tag{A5}$$

$$\frac{\partial q_p}{\partial t} = -\frac{1}{\overline{\rho}}\frac{\partial}{\partial x_i}(\overline{\rho} u_i q_p + F_{q_p i}) + \frac{1}{\overline{\rho}}\frac{\partial}{\partial z}(P_r + P_s + P_g) - \left(\frac{\partial q_p}{\partial t}\right)_{mic}, \tag{A6}$$

where $u_i (i = 1, 2, 3)$ are the resolved wind components u, v, w along the x, y, and vertical z directions, respectively; ρ is the air density; p is the pressure; h_L is liquid/ice water static energy; q_T is the total nonprecipitating water mixing ratio; q_p is the total precipitating water mixing ratio; f is the Coriolis parameter; B is the buoyancy; U_g is prescribed geostrophic wind; g is gravitational acceleration; c_p is specific heat at constant pressure; L_c and L_s are latent heat of evaporation and sublimation, respectively; τ_{ij} is subgrid-scale stress tensor; F_{h_L}, F_{q_T}, and F_{q_p} are subgrid-scale scalar fluxes; P_r, P_s, and P_g are rain, snow, and graupel precipitation fluxes, respectively; the subscript "rad" denotes the tendency due to radiative heating; "mic" represents the tendency of precipitating water due to conversion of cloud water/ice and due to evaporation; "l.s." denote the prescribed large-scale tendency; the overbar and prime represent the horizontal mean and perturbation from that mean, respectively. Further details about the microphysics and subgrid-scale parameterization in the model are presented in *Khairoutdinov and Randall* [2003].

Acknowledgments
We thank Marat Khairoutdinov and Filip Váňa for their work on the superparametrization configuration of IFS and Antje Weisheimer, Peter Bechtold, Frederic Vitart for discussions on ensemble superparameterization and tropical weather forecasts. We also would like to thank Glenn Carver for the OpenIFS support rendered for the superparametrization implementation in IFS. The authors received funding from an ERC grant (towards the Prototype Probabilistic Earth-System Model for Climate Prediction, project reference 291406). The model output data can be accessed on the ECMWF MARS data archive and will be made available upon request (e-mail: subramanian@atm.ox.ac.uk).

References

Ackerman, T. P., T. S. Cress, W. R. Ferrell, and J. H. Mather (2016), The programmatic maturation of the ARM Program, *Meteorol. Monogr.*, *57*, 3.1–3.19, doi:10.1175/AMSMONOGRAPHS-D-15-0054.1.

Andersen, J. A., and Z. Kuang (2012), Moist static energy budget of MJO-like disturbances in the atmosphere of a zonally symmetric aquaplanet, *J. Clim.*, *25*(8), 2782–2804.

Arakawa, A., and J. H. Jung (2011), Multiscale modeling of the moist-convective atmosphere—A review, *Atmos. Res.*, *102*(3), 263–285.

Arakawa, A., and W. H. Schubert (1974), Interaction of a cumulus cloud ensemble with the large-scale environment, Part I, *J. Atmos. Sci.*, *31*(3), 674–701.

Arakawa, A., and C. Wu (2013), A unified representation of deep moist convection in numerical modeling of the atmosphere, Part I, *J. Atmos. Sci.*, *70*(7), 1977–1992.

Arnold, N. P., Z. Kuang, and E. Tziperman (2013), Enhanced MJO-like variability at high SST, *J. Clim.*, *26*(3), 988–1001.

Arnold, N. P., M. Branson, Z. Kuang, and D. A. Randall (2015), MJO intensification with warming in the superparameterized CESM, *J. Clim.*, *28*, 2706–2724.

Bechtold, P., M. Köhler, T. Jung, F. Doblas-Reyes, M. Leutbecher, M. J. Rodwell, F. Vitart, and G. Balsamo (2008), Advances in simulating atmospheric variability with the ECMWF model: From synoptic to decadal time-scales, *Q. J. R. Meteorol. Soc.*, *134*, 1337–1351.

Berner, J., K. R. Smith, S. Y. Ha, J. P. Hacker, and C. Snyder (2015), Increasing the skill of probabilistic forecasts: Model-error representations versus calibration and debiasing, *Mon. Weather Rev*, *143*, 1295–1320.

Berner, J., et al. (2016), Stochastic parameterization: Towards a new view of weather and climate models, *Bull. Am. Meteorol. Soc.*, *98*, 565–588, doi:10.1175/BAMS-D-15-00268.1.

Blad, I., and D. L. Hartmann (1993), Tropical intraseasonal oscillations in a simple nonlinear model, *J. Atmos. Sci.*, *50*(17), 2922–2939.

Buizza, R., M. Milleer, and T. N. Palmer (1999), Stochastic representation of model uncertainties in the ECMWF ensemble prediction system, *Q. J. R. Meteorol. Soc.*, *125*(560), 2887–2908.

Charney, J. G. (1963), A note on large-scale motions in the tropics, *J. Atmos. Sci.*, *20*(6), 607–609.
Craig, G. C., and B. G. Cohen (2006), Fluctuations in an equilibrium convective ensemble: Part I: Theoretical formulation, *J. Atmos. Sci.*, *63*, 1996–2004.
Deng, Q., B. Khouider, and A. J. Majda (2015), The MJO in a coarse-resolution GCM with a stochastic multicloud parameterization, *J. Atmos. Sci.*, *72*(1), 55–74.
Emanuel, K. (1994), *Atmospheric Convection*, Oxford Univ. Press, Oxford, U. K.
Grabowski, W. W. (2003), MJO-like coherent structures: Sensitivity simulations using the cloud-resolving convection parameterization (CRCP), *J. Atmos. Sci.*, *60*(6), 847–864.
Grabowski, W. W., and P. K. Smolarkiewicz (1999), CRCP: A cloud resolving convection parameterization for modeling the tropical convecting atmosphere, *Physica D*, *133*(1–4), 171–178.
Grooms, I., and A. J. Majda (2013), Efficient stochastic superparameterization for geophysical turbulence, *Proc. Natl. Acad. Sci. U. S. A.*, *110*, 4464–4469.
Grooms, I., and A. J. Majda (2014), Stochastic superparameterization in quasigeostrophic turbulence, *J. Comput. Phys.*, *271*, 78–98.
Grooms, I., A. J. Majda, and K. S. Smith (2015), Stochastic superparameterization in a quasigeostrophic model of the Antarctic circumpolar current, *Ocean Modell.*, *85*, 1–15.
Hannah, W. M., and E. D. Maloney (2014), The moist static energy budget in NCAR CAM5 hindcasts during dynamo, *J. Adv. Model. Earth Syst.*, *6*(2), 420–440.
Hendon, H. H., and B. Liebmann (1990), The intraseasonal (30-50 Day) oscillation of the Australian summer monsoon, *J. Atmos. Sci.*, *47*(24), 2909–2923.
Hohenegger, C., and C. Schär (2007), Predictability and error growth dynamics in cloud-resolving models, *J. Atmos. Sci.*, *64*(12), 4467–4478.
Hohenegger, C., D. Lüthi, and C. Schär (2006), Predictability mysteries in cloud-resolving models, *Mon. Weather Rev.*, *134*(8), 2095–2107.
Houze, R. A. (2004), Mesoscale convective systems, *Rev. Geophys.*, *42*, RG4003, doi:10.1029/2004RG000150.
Hu, Q., and D. A. Randall (1994), Low-frequency oscillations in radiative-convective systems, *J. Atmos. Sci.*, *42*(4), 1089–1099.
Huffman, G. J., D. T. Bolvin, E. J. Nelkin, D. B. Wolff, R. F. Adler, G. Gu, Y. Hong, K. P. Bowman, and E. F. Stocker (2007), The TRMM multisatellite precipitation analysis (TMPA): Quasi-global, multiyear, combined-sensor precipitation estimates at fine scales, *J. Hydrometeorol.*, *8*(1), 38–55, doi:10.1175/JHM560.1.
Khairoutdinov, M., D. Randall, and C. DeMott (2005), Simulations of the atmospheric general circulation using a cloud-resolving model as a superparameterization of physical processes, *R. Meteorol. Soc. Interface*, *62*(7), 2136–2154.
Khairoutdinov, M. F., and Y. L. Kogan (1999), A large Eddy simulation model with explicit microphysics: Validation against aircraft observations of a stratocumulus-topped boundary layer, *J. Atmos. Sci.*, *56*(13), 2115–2131.
Khairoutdinov, M. F., and D. A. Randall (2003), Cloud resolving modeling of the ARM summer 1997 IOP: Model formulation, results, uncertainties, and sensitivities, *J. Atmos. Sci.*, *60*(4), 607–625.
Khouider, B., and A. J. Majda (2016), Models for multiscale interactions. Part i: A multicloud model parameterization, *Meteorol. Monogr.*, *56*, 9–1.
Kim, D., et al. (2009), Application of MJO simulation diagnostics to climate models, *J. Clim.*, *22*(23), 6413–6436.
Klein, R., and A. J. Majda (2006), Systematic multiscale models for deep convection on mesoscales, *Clim. Dyn.*, *20*(5–6), 525–551.
Kuo, H. L. (1965), On formation and intensification of tropical cyclones through latent heat release by cumulus convection, *J. Atmos. Sci.*, *22*(1), 40–63.
Leutbecher, M., and T. N. Palmer (2008), Ensemble forecasting, *J. Comput. Phys.*, *227*(7), 3515–3539.
Lewis, J. M. (2005), Roots of ensemble forecasting, *Mon. Weather Rev.*, *133*, 1865–1885.
Lin, J., and J. D. Neelin (2003), Toward stochastic deep convective parameterization in general circulation models, *Geophys. Res. Lett.*, *30*(4), 1162, doi:10.1029/2002GL016203.
Lin, J.-L., et al. (2006), Tropical intraseasonal variability in 14 IPCC AR4 climate models. Part I: Convective signals, *J. Clim.*, *19*(12), 2665–2690.
Lipps, F. B., and R. S. Hemler (1982), A scale analysis of deep moist convection and some related numerical calculations, *J. Atmos. Sci.*, *39*(10), 2192–2210.
Majda, A. J. (2007), Multiscale models with moisture and systematic strategies for superparameterization, *J. Atmos. Sci.*, *64*(7), 2726–2734.
Majda, A. J. (2012), Challenges in climate science and contemporary applied mathematics, *Commun. Pure Appl. Math.*, *65*(7), 920–948.
Majda, A. J., C. Franzke, and B. Khouider (2008), An applied mathematics perspective on stochastic modelling for climate, *Philos. Trans. R. Soc. London A*, *366*(1875), 2427–2453.
Maloney, E. D. (2009), The moist static energy budget of a composite tropical intraseasonal oscillation in a climate model, *J. Clim.*, *22*(3), 711–729.
Manabe, S., J. Smagorinsky, and R. F. Strickler (1965), Simulated climatology of a general circulation model with a hydrologic cycle, *Mon. Weather Rev.*, *93*(12), 769–798.
Mapes, B., S. Tulich, J. Lin, and P. Zuidema (2006), The mesoscale convection life cycle: Building block or prototype for large-scale tropical waves?, *Dyn. Atmos. Oceans*, *42*(1–4), 3–29.
Moncrieff, M. W. (1992), Organized convective systems: Archetypal dynamical models, mass and momentum flux theory, and parametrization, *Q. J. R. Meteorol. Soc.*, *118*(507), 819–850.
Neelin, J. D., and I. M. Held (1987), Modeling tropical convergence based on the moist static energy budget, *Mon. Weather Rev.*, *2*(5), 3–12.
Palmer, T. (2014), Build high-resolution global climate models, *Nature*, *515*(7527), 338–339.
Palmer, T. N. (2012), Towards the probabilistic Earth-system simulator: A vision for the future of climate and weather prediction, *Q. J. R. Meteorol. Soc.*, *138*(665), 841–861.
Palmer, T. N., F. J. Doblas-Reyes, and A. Weisheimer (2009a), Toward seamless prediction: Calibration of climate change projections using seasonal forecasts reply, *Bull. Am. Meteorol. Soc.*, *89*(4), 459–470.
Palmer, T. N., R. Buizza, F. Doblas-Reyes, T. Jung, M. Leutbecher, G. Shutts, M. Steinheimer, and A. Weisheimer (2009b), Stochastic parametrization and model uncertainty, *ECMWF Tech. Memo. 598*, Eur. Cent. for Medium-Range Weather Forecasts, Reading, U. K.
Peters, K., C. Jakob, L. Davies, B. Khouider, and A. J. Majda (2013), Stochastic behavior of tropical convection in observations and a multicloud model, *J. Atmos. Sci.*, *70*(11), 3556–3575.
Plant, R. S., and G. C. Craig (2008), A stochastic parameterization for deep convection based on equilibrium statistics, *J. Atmos. Sci.*, *65*(1), 87–105.
Plant, R. S., and J.-I. Yano (2015), *Parameterization of Atmospheric Convection*, vol. 1, World Sci., London.
Randall, D., M. Khairoutdinov, A. Arakawa, and W. Grabowski (2003), Breaking the cloud parameterization deadlock, *Bull. Am. Meteorol. Soc.*, *84*(11), 1547–1564.

Randall, D. A. (2013), Beyond deadlock, *Geophys. Res. Lett.*, *40*, 5970–5976, doi:10.1002/2013GL057998.
Raymond, D. J., and Ž. Fuchs (2009), Moisture modes and the Madden–Julian oscillation, *J. Clim.*, *22*(11), 3031–3046.
Shutts, G., and A. C. Pallarès (2014), Assessing parametrization uncertainty associated with horizontal resolution in numerical weather prediction models, *Philos. Trans. R. Soc. A*, *372*(2018), 20130284, doi:10.1098/rsta.2013.0284.
Shutts, G. J., and T. N. Palmer (2007), Convective forcing fluctuations in a cloud-resolving model: Relevance to the stochastic parameterization problem, *J. Clim.*, *20*(2), 187–202.
Slingo, J. M., et al. (1996), Intraseasonal oscillations in 15 atmospheric general circulation models: Results from an AMIP diagnostic subproject, *Clim. Dyn.*, *12*(5), 325–357.
Smagorinsky, J. (1960), On the dynamical prediction of large-scale condensation by numerical methods, in *Physics of Precipitation: Proceedings of the Cloud Physics Conference, Woods Hole, Massachusetts, June 3-5, 1959*, *Geophys. Monogr. Ser.*, edited by H. Weickmann, AGU, Washington, D. C.
Smith, R. K. (2013), *The Physics and Parameterization of Moist Atmospheric Convection*, vol. 505, Springer, Dordrecht, Netherlands.
Sobel, A., and E. Maloney (2013), Moisture modes and the eastward propagation of the MJO, *J. Atmos. Sci.*, *70*(1), 187–192.
Sobel, A. H., J. Nilsson, and L. M. Polvani (2001), The weak temperature gradient approximation and balanced tropical moisture waves, *J. Atmos. Sci.*, *58*(23), 3650–3665.
Subramanian, A., A. Weisheimer, T. Palmer, F. Vitart, and P. Bechtold (2016), Impact of stochastic physics on tropical precipitation in the coupled ECMWF model, *Q. J. R. Meteorol. Soc.*, *143*, 852–865, doi:10.1002/qj.2970.
Subramanian, A. C., and G. J. Zhang (2014), Diagnosing MJO hindcast biases in NCAR CAM3 using nudging during the dynamo field campaign, *J. Geophys. Res. Atmos.*, *119*, 7231–7253, doi:10.1002/2013JD021370.
Wang, Y., G. J. Zhang, and G. C. Craig (2016), Stochastic convective parameterization improves the simulation of tropical precipitation variability in the NCAR CAM5, *Geophys. Res. Lett.*, *43*, 6612–6619, doi:10.1002/2016GL069818.
Watson, P. A. G., H. M. Christensen, and T. N. Palmer (2015), Does the ECMWF IFS convection parameterization with stochastic physics correctly reproduce relationships between convection and the large-scale state?, *J. Atmos. Sci.*, *72*(1), 236–242.
Weisheimer, A., S. Corti, and T. Palmer (2014), Addressing model error through atmospheric stochastic physical parametrizations: Impact on the coupled ECMWF seasonal forecasting system, *Philos. Trans. R. Soc.*, *372*, 20130290, doi:10.1098/rsta.2013.0290.
Wolding, B. O., and E. D. Maloney (2015), Objective diagnostics and the Madden–Julian oscillation. Part II: Application to moist static energy and moisture budgets, *J. Clim.*, *28*(19), 7786–7808.
Xing, Y., A. J. Majda, and W. W. Grabowski (2009), New efficient sparse space-time algorithms for superparameterization on mesoscales, *Mon. Weather Rev.*, *137*(12), 4307–4324.
Yano, J.-I. (2016), Subgrid-scale physical parameterization in atmospheric modeling: How can we make it consistent?, *J. Phys. A*, *49*(28), 284001.